Article:
Bányai, L, Nagy, L, Hooper, A et al. (2020) Investigation of Integrated Twin Corner Reflectors Designed for 3-D InSAR Applications. IEEE Geoscience and Remote Sensing Letters, 17 (6). pp. 1013-1016. ISSN: 1545-598X

https://doi.org/10.1109/lgrs.2019.2939675

Investigation of Integrated Twin Corner Reflectors Designed for 3-D InSAR Applications

László Bányai, Lajos Nagy, Andrew Hooper, *Senior Member, IEEE*, István Bozsó, Eszter Szűcs, and Viktor Wesztergom

***Abstract*— There are potentially dangerous areas where InSAR technology cannot be applied routinely in the absence of proper persistent or distributed scatterers. Here, we planned and investigated the use of truncated trihedral triangle corner reflectors (CRs) oriented to ascending and descending directions for Sentinel-1 orbit, which were mounted on the optimal concrete basement including an additional global navigation satellite system (GNSS) adapter. These integrated benchmarks were designed to produce a signal-to-clutter ratio of about 100 (i.e., 20 dB). The mechanical design allows optimal orientation of the reflectors and resistance against dynamic effects. We investigated 1:5 models of the CRs and integrated benchmarks in an anechoic chamber to estimate the effects of truncation and the interference of the twin reflectors. The main effect of the interference is the asymmetric monostatic radar cross section, which can be neglected. The integrated benchmarks were also investigated in two recent landslide areas in Hungary using Sentinel-1 single look complex (SLC) scenes, which confirmed that the preliminary requirements can be met.**

***Index Terms*— Corner reflector (CR), InSAR, radar cross section (RCS), Sentinel-1, signal-to-clutter ratio (SCR).**

I. Introduction

ALTHOUGH the Sentinel-1 mission significantly improves the temporal and spatial coherence of SAR images, there are still important areas where rapid decorrelation means that InSAR technology cannot be used routinely. The installations of corner reflectors (CRs) can solve this problem if their signal-to-clutter ratio (SCR) is near to 100 (i.e., 20 dB) [1]. The SCR is defined by Freeman [2]

$$\mathrm{SCR} = \frac{\sigma_{\mathrm{pq}}^{T}}{\left\langle \sigma_{\mathrm{pq}}^{C} \right\rangle} \tag{1}$$

where σ_{pq}^{T} is the normalized point target radar cross section (RCS) and $\langle \sigma_{\mathrm{pq}}^{C} \rangle$ is the normalized average background clutter RCS.

Manuscript received May 7, 2019; revised August 9, 2019 and August 29, 2019; accepted August 31, 2019. This work was supported in part by European Space Agency, Plan for European Cooperating States (ESA PECS) through a project under Grant 4000114846/15/NL/NDe, in part by the National Excellence Program under Grant 2018-1.2.1-NKP-2018-00007, and in part by Research, Development and Innovation Fund through the Thematic Excellence Program under Grant TUDFO/51757/2019-ITM. *(Corresponding author: István Bozsó.)*

L. Bányai, I. Bozsó, E. Szűcs, and V. Wesztergom are with the Geodetic and Geophysical Institute, MTA CSFK, 9400 Sopron, Hungary (e-mail: banyai.laszlo@csfk.mta.hu; bozso.istvan@csfk.mta.hu; szucs.eszter@csfk.mta.hu; wesztergom.viktor@csfk.mta.hu).

L. Nagy is with the Department of Broadband Infocommunications and Electromagnetic Theory, BME HVT, 1111 Budapest, Hungary (e-mail: nagy@mht.bme.hu).

A. Hooper is with the COMET, School of Earth and Environment, University of Leeds, Leeds LS2 9JT, U.K. (e-mail: a.hooper@leeds.ac.uk).

Digital Object Identifier 10.1109/LGRS.2019.2939675

The SCR depends on several parameters, e.g., terrain type, vegetation density, soil moisture, radar wavelength, incidence angle, polarization, and SAR resolution. The clutter on flat cultivated terrain with low vegetation density is assumed to be between −10 and −12 dB [3].

The SCR is often computed from the actual SAR images as the ratio of the normalized peak power in the target impulse respond to the mean background clutter power, estimated from an area located close to the target [2].

The line-of-sight (LOS) error is related to the signal-to-clutter-ratio by Savio *et al.* [1]

$$\sigma_h = \frac{\lambda}{4\pi}\sqrt{\frac{1}{2\ \mathrm{SCR}}}. \tag{2}$$

The SCR of 100 (i.e., 20 dB) is an acceptable practical requirement, which gives $\sigma_h = 0.3$ mm using $\lambda = 5.5466$ cm as the wavelength of Sentinel-1 satellites. Moreover, the LOS phase accuracy in InSAR applications depends on several parameters, e.g., thermal noise, ionospheric effects, atmospheric phase screen, orbit and terrain elevation errors [4].

According to [1], the 2-D displacement vectors can be estimated by InSAR with millimeter accuracy using CRs. In [1], dihedral CRs with 1-m edge were chosen for ENVISAT and RADARSAT (S3) measurements to validate the accuracy of InSAR while in [3], trihedral triangle CRs with 1.5-m edge were chosen using TerraSAR-X, COSMO-SkyMed, RADARSAT-2, and RISAT-1 images for interferometric calibration and practical applications. The RCS of these CRs satisfied the practical SCR requirement as well.

The trihedral triangular CRs with 1-m edge have optimal properties and are recommended for practical applications by Ferretti [5]. The RCS of the trihedral triangular CRs is computed from

$$\mathrm{RCS} = \frac{4\pi L^4}{3\lambda^2}. \tag{3}$$

$L = 1$ m and $\lambda = 5.5466$ cm give RCS $= 1361.6$ m^2 (i.e., 31.3 dB m^2). The error sources of the manufactured CRs are the surface irregularities and orthogonality errors [3], [6]. If the surface irregularities (< 1 mm) and interplate orthogonality errors ($< 1°$) result in -1.3 dB m^2 loss, thus 1000 m^2 (i.e., 30 dB m^2) RCS can be practically provided.

Since the three-tip areas of trihedral triangle CRs are outside of the illuminated region, they can be removed. The removal does not reduce the maximum RCS, but this CR is significantly less sensitive to the unwanted coherent ground

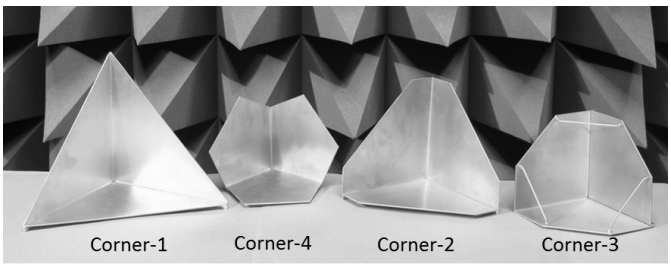

Fig. 1. Investigated 1:5 ratio CRs (Corner-1: triangle, Corner-4: self-illuminating, Corner-2: 20% truncated, and Corner-3: 33% truncated with anchors).

interactions and its size and surface are significantly smaller. CRs that retain only the illuminated regions are known as "self-illuminating" or "hexagonal" reflectors [7], [8].

In the main part of this letter, we summarize the mechanical design and the necessary electromagnetic investigations of our integrated geodetic/geodynamic benchmarks (IBs) that are needed to validate their practical applications. The results are confirmed by Sentinel-1 single look complex (SLC) images of test networks.

II. Mechanical Design of Integrated Benchmarks

We have designed IBs, which consist of twin radar reflectors oriented to ascending (ASC) and descending (DSC) directions, respectively, together with geodetic reference marks, which allow the direct combinations of InSAR and global navigation satellite system (GNSS) technologies. The coordinates of the geodetic reference adapters can be measured by GNSS technology and the relative positions of the CR phase centers can be measured as well. The LOS phase differences computed from two GNSS measurement can be used in the combined data processing.

For practical applications, trihedral triangle CRs with 1-m edge were chosen, which provide in Sentinel-1 *C*-band an RCS of about 1000 m^2 (i.e., 30 dB m^2) and can achieve an SCR of about 100 (i.e., 20 dB).

Very precise, but sophisticated and expensive, CRs were manufactured that can be oriented toward different SAR satellite orbits [1], [3]. We applied only three parallel legs headed by rotating junctions with changeable length and rotational freedom in two axes, the third rotating axis is provided by changing the heights of the legs. The junctions are fixed to the CR's ground plane and the legs are cemented in a rigid basement. Using this method aided by a magnetic compass and a simple tilt meter produces adequate Sentinel-1 LOS orientation.

From a geodetic point of view, the phase centers and the adapter for GNSS measurements should be as close as possible, which constrains the surface area of the basement. From a practical point of view, a 1 m^2 surface is an economical choice. Trihedral triangle CRs with 1-m edge cannot be applied on this surface even if they are in a face-to-face arrangement. Self-illuminating CRs are the smallest but the necessary closeness of the three legs and the connections of the three sides are mechanically less rigid.

The truncation of 20% along and perpendicular to the three 1-m edges still preserves the rigidity of the CRs and it means

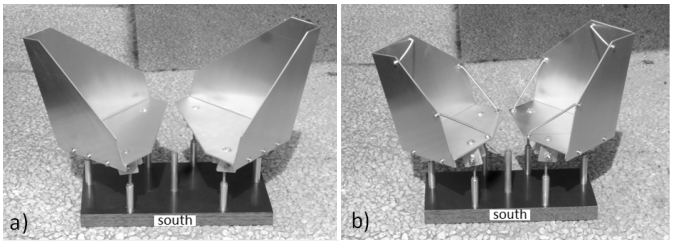

Fig. 2. Investigated 1:5 ratio face-to-face IBs. (a) 20% truncated. (b) 33% truncated (the central rod is the GNSS adapter).

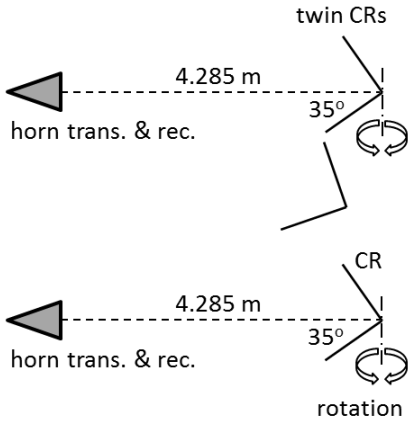

Fig. 3. Measurement scenarios for twin and single CR investigation. The dashed "horizontal" line is the direction of maximum reflectivity. The rotation is about the "vertical" dashed line.

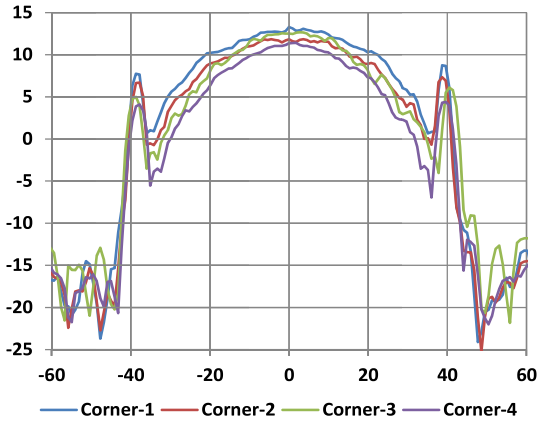

Fig. 4. Monostatic RCS [dB m^2] of investigated CRs versus horizontal angle [degree], 0° is related to maximum reflectivity.

that they can be placed on a 1.0 m^2 surface in a face-to-face arrangement. The truncation of 33% along and perpendicular to the three 1-m edges still preserves the illuminated areas and it means that they can be placed on a 0.7 m^2 surface in a face-to-face arrangement. To strengthen the CRs, additional anchors were applied outside of the illuminated areas.

III. Electromagnetic Investigation of Designed Reflectors

The dependence of RCS on viewing angles can be numerically simulated or measured in anechoic chambers using properly scaled models. Our measurements were carried out in the anechoic chamber of the Department of Broadband

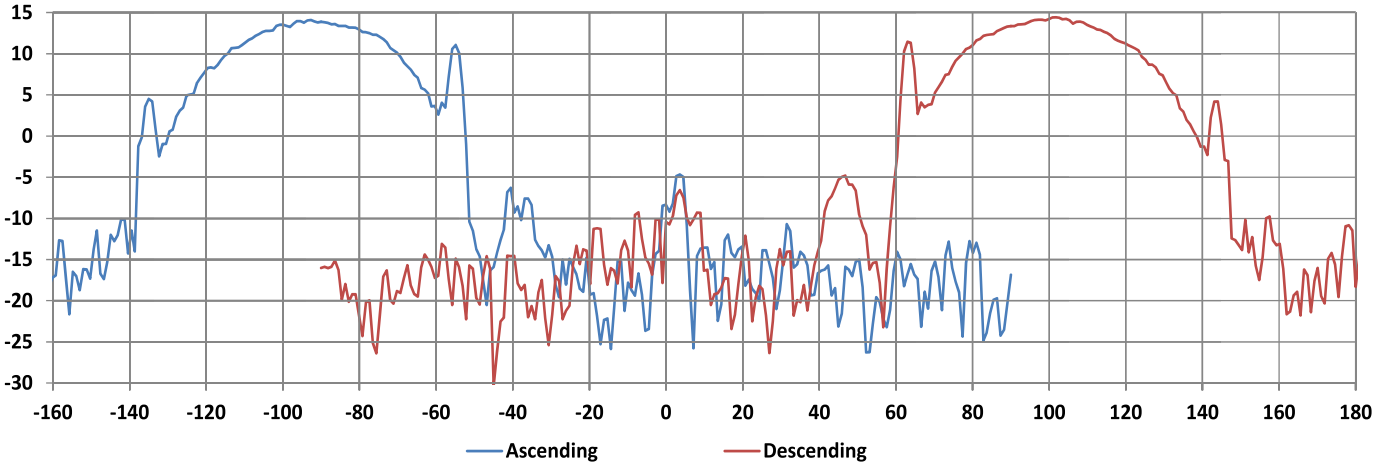

Fig. 5. Monostatic RCS [dB m^2] of 20% truncated IB versus horizontal angle [degree], 0° is related to north direction.

Infocommunications and Electromagnetic Theory, Budapest University of Technology and Economics.

The devices used were an Agilent N523A vector network analyzer, an HP859E spectrum analyzer, an RFT 02012 antenna rotary unit, an HP E3631A power supply, a DellXPS15z PC, and an Agilent 82357B Universal Serial Bus (USB)-general purpose interface bus (GPIB) interface.

According to the available space in the anechoic chamber, the investigated CRs (Fig. 1) and IBs (Fig. 2) were scaled at 1:5 and a measurement frequency of 27 GHz (5 × 5.4 GHz) was used with 7-dBm transmit power. Since the reflectivity cannot be five times exaggerated, $L = 0.2$ m and $\lambda = 1.1103$ cm give only RCS = 54.4 m^2 (i.e., 17.35 dB m^2). Moreover, the comparisons of different curves are very useful.

The measurement scenario is shown in Fig. 3, where the angle between the line of maximum reflectivity (in this case horizontal) and the ground plane is 35°. The CRs and IB models are rotated about the vertical axis to simulate the relative satellite motion. The measured RCS dependence on a horizontal angle is shown in Fig. 4. The symmetric behavior of the different CRs is very similar. The peak maximum between the theoretical and measured RCS differs by about 3–4 dB m^2. It is a consequence of the individual CRs and the measurement errors caused by instrumentation, finite measurement distance, isolation between transmit and receive direction, and background reflection of the chamber wall. The differences are real.

Our two models of IBs were also investigated. The effect of DSC CRs on ASC CRs and vice versa was measured in the same way. Since the results of both models (20% and 33% truncated) are very similar, only the 20% truncated is shown in Fig. 5, which, as compared with Fig. 4, clearly indicates the asymmetry of RCS curves in both ASC and DSC directions. The ASC and DSC CRs of the model (and practical) IBs are oriented according to the computed satellite directions. The azimuths are asymmetric to the north-south direction and the incidence angles are also different. The twin arrangement and the asymmetric directions are the main reasons for RCS

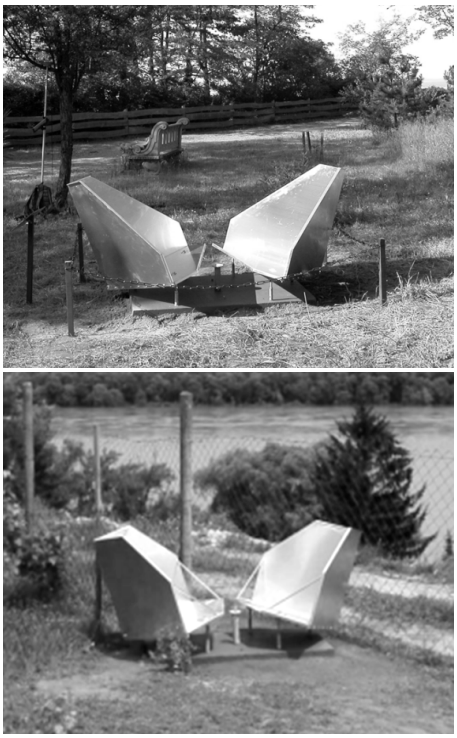

Fig. 6. Manufactured face-to-face IBs [(Top) 20% truncated and (Bottom) 33% truncated]. The central rod is the GNSS adapter.

distortions, which can be neglected in angular width region of ±5°.

The phase center offset of real twin arrangement can be estimated only by numerical calculations using e.g., CST Microwave Studio using the asymptotic solver, which is based on the extended physical optic approximation. The offset can be explained by the same factors as RCS asymmetry.

These offsets can be handled as displacements or can be canceled by LOS differencing between the stable and moving CRs [1], [4]. Our estimated offsets (1.7 mm along the "ground" edges and 0.6 mm along the "vertical" edge) are very small.

TABLE I

AVERAGE SCR OF PIXELS DOMINATED BY 20% TRUNCATED CRS. σ^T_{PQ} IS A PEAK POWER AND $\langle\sigma^C_{\mathrm{PQ}}\rangle$ IS A MEAN BACKGROUND POWER

IB	ascending			descending		
	σ^T_{pq}	$\langle\sigma^C_{pq}\rangle$	SCR	σ^T_{pq}	$\langle\sigma^C_{pq}\rangle$	SCR
IB1	8.347	0.074	113 (21 dB)	8.832	0.071	125 (21 dB)
IB2	11.061	0.065	171 (22 dB)	7.545	0.097	78 (19 dB)
IB3	9.567	0.055	175 (22 dB)	10.735	0.094	115 (21 dB)
IB4	8.742	0.058	151 (22 dB)	10.345	0.097	110 (20 dB)

TABLE II

AVERAGE SCR OF PIXELS DOMINATED BY 33% TRUNCATED CRS. σ^T_{PQ} IS A PEAK POWER AND $\langle\sigma^C_{\mathrm{PQ}}\rangle$ IS A MEAN BACKGROUND POWER

IB	ascending			descending		
	σ^T_{pq}	$\langle\sigma^C_{pq}\rangle$	SCR	σ^T_{pq}	$\langle\sigma^C_{pq}\rangle$	SCR
AR	7.781	0.099	79 (19 dB)	6.497	0.099	66 (18 dB)
A1	5.381	0.089	60 (18 dB)	6.258	0.098	63 (18 dB)
A2	7.019	0.077	91 (20 dB)	8.400	0.103	81 (19 dB)
A3	8.661	0.066	132 (21 dB)	8.174	0.100	82 (19 dB)
A4	5.803	0.057	102 (20 dB)	7.084	0.085	83 (19 dB)

IV. PRACTICAL CONFIRMATIONS

The two types of manufactured IBs (Fig. 6) were used in two different landsliding test networks. Between April and November 2017, 31 ASC and 36 DSC Sentinel-1A and 1B SLC images were analyzed in both areas. The normalized power images were computed by the Gamma DIFF&GEO modules [9]. Approximately 100×100 m square area around our IBs were analyzed. The pixels that were dominated by local maximums were deleted and the remaining pixels were used to estimate the mean background clutter power. The estimated and averaged SCR values are summarized in Table I (Dunaszekcső) and in Table II (Kulcs).

The SCR values vary between 63 (i.e., 18 dB) and 175 (i.e., 22 dB) which correspond to $\sigma_h = 0.2$ mm and $\sigma_h = 0.4$ mm LOS error, respectively.

Since the LOS errors are well below 1 mm, the results are practically satisfactory. The differences are due to the estimated varying background clutter which depends on several parameters mentioned in the introduction.

V. CONCLUSION

Electromagnetic investigations and practical confirmations were carried out to investigate the usefulness of integrated benchmarks designed for integrated applications of GNSS and InSAR technologies, equipped with optimally truncated ASC and DSC CRs. IB designs with both 20% truncated and 33% truncated CRs have similar RCS characteristics, but the design with 33% truncated CRs can be placed on a 0.7 m^2 concrete surface, which makes benchmark installment more economic in rugged terrains. The interference of a face-to-face arrangement does not significantly affect the maximum reflectivity in the acceptable angular width region. The phase center offsets can be canceled by LOS differencing or can be computed by numeric simulations.

In summary, two designs of IBs that we investigated satisfy the expected practical requirements and behave as excellent persistent scatterers in the test areas.

If there are Sentinel-1 images available, it is advisable to estimate the background reflectivities during the selection of the observation sites as well.

REFERENCES

[1] G. Savio, A. Ferretti, F. Novali, S. Musazzi, C. Prati, and F. Rocca, "PSInSAR validation by means of a blind experiment using dihedral reflectors," in *Proc. Fringe Workshop*, Frascati, Italy, Nov./Dec. 2005, p. 6.

[2] A. Freeman, "SAR calibration: An overview," *IEEE Trans. Geosci. Remote Sens.*, vol. 30, no. 6, pp. 1107–1121, Nov. 1992.

[3] M. C. Garthwaite, S. Nancarrow, A. Hislop, M. Thankappan, J. H. Dawson and S. Lawrie, "The design of radar corner reflectors for the Australian Geophysical Observing System," *Geosci. Aust. Rec.*, vol. 3, p. 86, Mar. 2015.

[4] R. F. Hanssen, *Radar Interferometry: Data Interpretation and Error Analysis*. New York, NY, USA: Kluwer, 2002, p. 308.

[5] A. Ferretti, *Satellite InSAR Data: Reservoir Monitoring From Space*. Houten, The Netherlands: EAGE, 2014, p. 159.

[6] M. Zink and H. Kietzmann, "Next generation SAR—External calibration," German Aerosp. Center, Cologne, Germany, Tech. Rep. 95-41, 1995, p. 45.

[7] K. Sarabandi and T.-C. Chiu, "Optimum corner reflectors for calibration of imaging radars," *IEEE Trans. Antennas Propag.*, vol. 44, no. 10, pp. 1348–1361, Oct. 1996.

[8] E. F. Knott, *Radar Cross Section Measurements*. Raleigh, NC, USA: SciTech, 2006.

[9] C. Werner, U. Wegmüller, T. Strozzi, and A. Wiesmann, "Gamma SAR and interferometric processing software," in *Proc. ERS-ENVISAT Symp.*, Gothenburg, Sweden, Oct. 2000, pp. 1–9.